



Adsorption of Crystal Violet Dye on Biomass from *Bauhinia tomentosa* Seed Pod Powder: Equilibrium and Kinetic Studies

K. Poonkodi^{1*}, V. Anitha², R. Chitradevi², M. Suganthi³, K. Vimaladevi⁴, V. Prabhu⁴, R. Mini⁴ and M. Anusuya⁴

¹Assistant Professor and Head, Post Graduate Department of Chemistry, Nallamuthu Gounder Mahalingam College, Pollachi, Coimbatore, Tamil Nadu, India

²Assistant Professor, Department of Chemistry, Sri G.V.G Visalakshi College for Women, Udumalpet, Tiruppur, Tamil Nadu, India

³Assistant Professor and Head, Department of Chemistry, Dr.N.G.P Arts and Science College, Coimbatore, Tamil Nadu, India

⁴Assistant Professor, Department of Chemistry, Nallamuthu Gounder Mahalingam College, Pollachi, Coimbatore, Tamil Nadu, India

Received: 11 Sep 2022

Revised: 06 Oct 2022

Accepted: 08 Nov 2022

*Address for Correspondence

K. Poonkodi

Assistant Professor and Head,
Post Graduate Department of Chemistry,
Nallamuthu Gounder Mahalingam College,
Pollachi, Coimbatore, Tamil Nadu, India
Email: Poonks.che@gmail.com



This is an Open Access Journal / article distributed under the terms of the **Creative Commons Attribution License** (CC BY-NC-ND 3.0) which permits unrestricted use, distribution, and reproduction in any medium, provided the original work is properly cited. All rights reserved.

ABSTRACT

The purpose of the current work is to explore the adsorptive removal of Crystal violet dye using a green adsorbent prepared from *Bauhinia tomentosa* seed pods (BTSP). The adsorbent was characterized by the use of FT-IR, XRD, EDAX and SEM studies. To evaluate the synthesized activated carbon's adsorption effectiveness, batch mode adsorption was used. The effect of pH, contact time, reaction temperature and adsorption dosage were tested. The experimental data were evaluated using Freundlich, Langmuir and Tempkin adsorption isotherms. Pseudo-first-order, pseudo-second-order, Elovich, and intraparticle diffusion models were used to assess the adsorption reaction's kinetics. The percentage removal of CV dye increases with the increase of pH, an increase in time, an increase in temperature and an increase in adsorbent dosage. The data were well fitted with Langmuir adsorption, which demonstrated that the elimination of CV dye followed the monolayer adsorption isotherm. The ideal pH range was 4 to 9, and the adsorption equilibrium was attained in 70 minutes. Pseudo-second-order and Elovich models successfully predicted the Crystal violet dye removal procedure. According to the results, the low-cost adsorbent made from *B. tomentosa* shows a high potential for removing dye from an aqueous solution.



**Poonkodi et al.,**

Waste seed pods can be utilized in large-scale dye removal since they are an excellent, low-cost alternative to commercial adsorbents.

Keywords: Adsorption, Crystal violet, *Bauhinia tomentosa*, Equilibrium and kinetics.

INTRODUCTION

In recent years, man-made synthetic chemicals have become more prevalent in the environment. Poor disposal practices and insufficient measures to manage harmful effluents from various sectors have resulted in widespread contamination of surface water and ground water. Synthetic dyes are used by numerous major industries, like paper, plastic, cosmetics, textiles, and food, to colour their products [1]. The most evident sign of water pollution is colour; when coloured debris is dumped into streams, it not only detracts from their aesthetic appeal but also prevents sunlight from reaching the streams, which affects photosynthesis [2]. It is highly noticeable and undesirable when relatively minute levels of dyes are present in water [3]. Some colours are mutagenic and can cause cancer [4]. The Proper treatment of waste water is crucial due to the numerous negative impacts, and while many effective technologies are already in use, alternative low-cost and readily accessible adsorbents are still required. One of the most widely distributed plants, *Bauhinia tomentosa* is utilized as ornamental purpose and has many medicinal uses. The seed pods can be employed as a green adsorbent for the treatment of waste water and are freely available. From the literature, there is no report on the green adsorbent prepared from *B. tomentosa* seed pod, the present study aimed to evaluate the adsorptive removal of Crystal violet by green adsorbent prepared from *B. tomentosa* seed pods and its equilibrium and kinetics studies.

MATERIALS AND METHODS

Preparation of adsorbent

Ripened *B. tomentosa* seed pods (BTSP) were collected in Samathur, Tamilnadu, India. The pods were cleaned with water to remove any dust particles, cut into small pieces, and then dried for a total of 10 days in the sun and another 24 hours in a hot air oven at 60°C. The material powdered up well after being fully dried. The powdered raw material was chemically activated by treating it with Conc. Sulphuric acid (1:2) with constant stirring and kept it for 24 hours. The resulting carbonized material was thoroughly cleaned with plenty of water, rinsed multiple times with distilled water to bring the pH level down to 7 and then dried at 105°C to 110°C in a hot air oven. The resulting adsorbent was thoroughly crushed, sieved through 210 mesh, labelled (BTSP), and stored in an airtight container for later use.

Adsorbate Solution

The adsorbate, Crystal Violet is a monovalent cationic triphenyl methane dye, the stock solution was prepared by dissolving 1g of Crystal Violet dye (AR) in distilled water and diluted to 1000 ml (1ppm). The stock solution was diluted to appropriate concentrations. The initial pH was adjusted with 0.1 M HCl or 0.1M NaOH.

Adsorbent Characterization

Scanning Electron Microscopy (SEM) and Energy Dispersive Analysis of X-Ray (EDAX) were used to evaluate the surface morphology of BTSP at the microscopic level. BTSP's crystalline structure was assessed using an X-ray diffract meter (XRD). Fourier Transform Infrared Spectroscopy was used to examine the functional groups that were present on the surface of BTSP.

Adsorption experiments

Batch mode experiments were performed to study the effect of various parameters such as contact time, pH, adsorbent dose, and temperature affecting the adsorptive removal of CV dye. In the adsorption experiments, 100 ml





Poonkodi et al.,

of the dye solutions of the desired concentration and pH were taken in a conical flask containing pre-determined weighed amounts of adsorbent (50mg). The conical flask containing adsorbent and adsorbate was equilibrated by shaking the contents at room temperature using a thermostat coupled rotary shaker (120 rpm) for different time intervals (10, 20, 30, 40, 50, 60, and 70 minutes). Then the solutions were filtered using filter paper and the filtrates were analyzed for the residual CV dye concentration using a UV spectrometer at a wavelength of 591 nm.

$$\% \text{ removal of CV dye} = \frac{C_0 - C_e}{C_0} \times 100 \quad (1)$$

Where, C_0 and C_e (mg/L) are the initial and equilibrium concentration of CV dye respectively. The amount of dye adsorbed at equilibrium (q_e) was calculated from the following equation.

$$q_e = \frac{(C_0 - C_e) \times V}{M} \quad (2)$$

Where q_e is the amount of dye adsorbed at equilibrium (mg/g). C_0 and C_e (mg/L) are the initial and equilibrium concentration of CV dye respectively. V is the volume of the solution (L) and M is the mass of the adsorbent used (g).

Adsorption isotherm studies

The adsorption isotherm models generally design and comprehend the mechanism of interaction between adsorbate and the adsorbent at equilibrium (Hameed et al, 2008). The Freundlich model implies heterogeneous energy distribution of active sites, while the Langmuir model assumes monolayer adsorption on a physically homogeneous adsorbent.

Langmuir equation

$$\frac{C_e}{q_e} = \frac{1}{q_m K_L} + \frac{C_e}{q_m} \quad (3)$$

Freundlich equation

$$\log q_e = \log k_f + \frac{1}{n} \log C_e \quad (4)$$

Tempkin isotherm

$$q_e = B \ln A + B \ln C_e \quad (5)$$

Where, q_e (mg/g) is the amount of dye adsorbed per unit weight of adsorbent, C_e (mg/L) is the concentration of dye solution at equilibrium, k_f (mg/g) and n are the Freundlich constants that indicate the adsorption capacity and intensity of adsorption respectively.

Adsorption kinetics

Kinetic studies are carried out to provide information about the mechanism of adsorption.

Pseudo- first –order kinetic [5]

$$\log (q_e - q_t) = \log q_e - k_1 t / 2.303 \quad (6)$$

Where q_e and q_t (mg/g) are the amounts of dye adsorbed at equilibrium and at time t and k_1 (1/min) are the rate constant of the pseudo -first order adsorption

Pseudo- second – order kinetic [6]

$$t / q_t = 1 / K_2 q_e^2 + t / q_e \quad (7)$$

K_2 (g mg⁻¹ min⁻¹) is the rate constant of pseudo -second order adsorption



Poonkodi *et al.*,**Elovich kinetic model**

$$q_t = 1/\beta \ln(\alpha\beta) + 1/\beta \ln t \quad (8)$$

The parameter β (g mg^{-1}) is related to the extent of the surface coverage and activation energy for chemisorptions [7,8]. The values of α and β can be calculated from the plot of q_t against $1/\ln t$.

RESULTS AND DISCUSSION**FT-IR Analysis**

The functional groups present in the raw powder, before and adsorption of CV dye onto BTSP were presented in Fig.1a,b & c. The broad peak appeared in raw powder responsible for -OH and -NH stretching at $3200\text{-}3500\text{cm}^{-1}$, a sharp peak at 2800cm^{-1} was attributed to C=C symmetrical stretching, another sharp peak at 1670 cm^{-1} was due to C=O carbonyl stretching frequencies. From the IR results the *B.Tomentosa* seed pod contains many phytochemicals especially carboxylic acids, phenolic compounds, alcohol or amine compounds [9]. After carbonization, the peak intensity of -OH and C=C stretching was reduced. But After the adsorption of CV dye onto BTSP, the -OH and C=O stretching disappeared, this may be due to the adsorption of dye molecule by these two active functional groups.

Scanning Electron Microscopic (SEM) studies

Figure 2 displays scanning electron microscopic images of the adsorbent BTSP both before and after Crystal violet dye adsorption. The image demonstrated the huge active cavities in the activated carbon made from *B. tomentosa* plant seed pods. These cavities are particularly helpful for adsorbing the dye molecules, as shown by the SEM image after adsorption, which revealed a reduction in cavity size from 50 to 5 μm . This illustrates the efficiency of a prepared adsorbent.

EDAX Analysis

Based on the EDAX results, the elementary analysis of the BTSP fruit shell before adsorption are presented in Fig.3. The elements and their % mass were listed in Table 1. High levels of carbon served as an effective adsorbent.

X-ray diffraction analysis

The adsorbent can be crystallographically characterized by means of XRD. The XRD pattern of the adsorbents showed the typical spectrum having main and secondary peaks at around ($2\theta=24^\circ, 64^\circ$) respectively. The results showed that the adsorbent has more pore structures and resembles with graphitic carbon [10].

BATCH MODE ADSORPTION STUDIES**Effect of contact time on the adsorption of CV on to BTSP**

As reaction time increased, the amount of dyes adsorbed also increased [11]. At an ideal initial concentration (100ppm and 150ppm), studies were conducted to determine the impact of contact time on the removal of CV dye [12]. The elimination of CV was 98.42% in 100 ppm and 99.06 % in 150 ppm. Fig. 4a shows the impact of the length of time the adsorbent and adsorbate were in contact. According to the findings, the adsorption of dye increased with longer shaking times and reached equilibrium at a constant value after a certain amount of time (70min). Additionally, it was shown that the dye's uptake began quickly during the first few minutes of contact time, increased gradually until it reached equilibrium, and then stabilized there. In addition, Fig. 4a probable monolayer covering of dye on the carbon surface was suggested by continual increase in adsorption, which eventually reached saturation [3].

Effect of adsorbent dose on the adsorption of CV onto BTSP

The effect of adsorbent dose was also tested for the removal of all the dyes from the aqueous solution. 100 ml of an aqueous dye solution and an adsorbent dosage ranging from (10 mg to 70 mg) were used to conduct the experiments [13]. The results, which are displayed in Fig.4b, demonstrated that dye removal efficacy increased with increasing





Poonkodi *et al.*,

amount of BTSP. To put it another way, dye removal was dose-dependent. In 70 mg of BTSP, the elimination of CV was 100% for 100ppm and 98.77% for 150ppm. The increase in adsorption with the addition of more adsorbent can be attributed to the availability of more adsorption sites and an increase in adsorption surface [14,15]. The addition of more binding sites for adsorption led to an increase in the elimination of dyes with increased adsorbent dose [13]. Beyond 70 mg/l, increasing the adsorbent dosage didn't significantly improve the efficiency.

Effect of pH on the adsorption of CV onto BTSP

In both chemical and biological interactions, the pH factor is extremely important. The amount of electrostatic charges that are imparted by the ionised dye molecules and the charges on the surface of the adsorbent are controlled by the pH of a medium [16]. Fig. 5a evaluated how pH affected the adsorptive removal of CV dye from BTSP. At pH 9, the greatest amount of elimination was seen (92.75 for 100 ppm & 94.36 for 150 ppm). Due to the large concentration of H⁺ ions, which create repulsion and hence diminish biosorption at lower pH levels, CV biosorption was low at lower pH levels [17]. There are more negatively charged surfaces accessible when the pH rises, which causes the attraction between the positively charged dye molecule and the biosorbent to weaken [5].

Effect of temperature on the adsorption of CV onto BTSP

In order to determine the impact of temperature on the percentage of CV dye removed by BTSP adsorbent, experiments were performed at various temperatures for 100ppm and 150ppm dye concentrations (35.5 to 43.5°C). The findings are shown in Fig. 5b. As the temperature increased, the rate of adsorption removal also increased, reaching a maximum at 97.9° C for 100 ppm and 99.53° C for 150 ppm [13]. This can be explained by the fact that the reduction in solution viscosity caused by an increase in temperature speeds up the diffusion of adsorbate molecules through the exterior boundary layer and into the internal pores of the adsorbent particles [18]. Furthermore, the mobility or collision of the adsorbate support molecules increases with temperature, which also raises the quantity of active sites on the adsorbent [22].

Adsorption kinetics for the adsorption of CV onto BTSP

Pseudo first order kinetic model

For various dye concentrations, linear plots of $\log(q_e - qt)$ vs. t were obtained (100 and 150 ppm). As a result, the adsorption process followed the first order rate expression (Fig.6a). The basic dye adsorption rate constants were observed to be (0.0112 and 0.0017 1/min). The regression coefficient (R²) of linear plots of pseudo-first order values was chosen as (0.944 & 0.939) for 100 & 150 ppm, respectively. When pore diffusion limits the adsorption process, However the relationship between initial solute concentration and rate of adsorption will not be linear.

Pseudo- second –order kinetic model

If second-order kinetics is used, the plot of t/qt versus t shows a linear relationship. As shown in Fig. 6b, (t/qt vs. t) is a straight line. For 100 and 150ppm, the K₂ values are (0.004 & 0.002), respectively. The plot's slopes and intercepts determine the k₂ and q_e values. The best fit model was chosen because the values of the regression coefficient (R²) of linear plots of pseudo-second order are (0.999 & 0.973) for 100 and 150ppm, respectively. The linear plot revealed a high degree of agreement between the experimental and calculated q_e values for CV adsorption onto BTSP. The best correlation for the system was provided by the pseudo-second-order model, which suggested that chemical adsorption might involve valency forces via electron sharing or exchange between adsorbent and adsorbate [4]. This phenomenon could be explained in two stages: first, the concentration gradient drove the CV ions to access or enter the pores of the adsorbent; second, the CV ions did not diffuse into the pores of pirina for further reactions until the surface functional sites were fully occupied [19].

Elovich kinetic model

Adsorption also followed the Elovich model, a plot of qt vs $\ln t$ should yield a linear relationship with slope of (1/b) and an intercept of (1/b) $\ln(a/b)$ [20]. The Elovich plot $\ln T$ vs qt was shown in fig 6c. The R² values are (0.973 & 0.944) for 100 and 150 ppm respectively. Pseudo second order results are in similar to that of Elovich model, thus indicating that the dynamic uptake of crystal violet can be best interpreted by the pseudo second-order model. It can





also be seen that the experimental equilibrium sorption values, obtained for 100 ppm & 150 ppm dye solutions are in close agreement with the theoretical values. The corresponding correlation coefficient (R^2) values for the pseudo-second order kinetic model was 0.999 in 100 ppm & 0.973 150 ppm, indicated the applicability of the pseudo-second order kinetic model which described the adsorption process of CV onto BTSP. It revealed that the pseudo-second order kinetic model provided good correlation for the adsorption. The higher R^2 values confirmed that the sorption process of CV onto BTSP follow a pseudo-second order kinetic model. Similar trends were observed for dye adsorption onto *Zea mays* [21]. It was suggested that the adsorption was controlled by chemisorptions [22]. Comparison of the correlation coefficients of kinetic parameters for the adsorption of CV onto BTSP was given in table. 2

Adsorption Isotherms for the Adsorption of CV on to BTSP

Langmuir Adsorption Isotherm

The values of K_L and b were determined from the slope and intercept of the plot. The K_L values were found in the range (0.2032 & 0.1459) for 100 ppm and 150 ppm, respectively indicated favourable adsorption of CV onto BTSP given the Table 3. When showed the values of C_e and C_e/q_e . The graph is plotted between C_e vs C_e/q_e the linear line show the figure 7a & b. The maximum adsorption corresponds to a saturated monolayer of adsorbate on the adsorbent surface with constant energy.

Freundlich Adsorption Isotherm

A plot of $\log q_e$ versus $\log C_e$ (Fig 8a & b) enabled us to determine the constant K_f and $1/n$. K_f is the indicator of the adsorption capacity, related to the bond energy and $1/n$ is the adsorption intensity of dye onto the adsorbent or surface heterogeneity. The magnitude of the exponent, $1/n$, gives an indication of favourable adsorption. Value of $1/n < 1$ represent a favourable adsorption condition while $1/n > 1$ is indicative of cooperative adsorption [6]. The K_f values were found in the range (1.8757 & 2.0218) for 100 ppm and 150 ppm and $1/n$ values are (0.1270 & 0.1830) for 100 ppm and 150 ppm. The graph is plotted $\log C_e$ vs $\log C_e/q_e$ the linear line was obtained and given in the (Fig 8 a & b).

Tempkin isotherm

Tempkin isotherm takes into account adsorbing species- adsorbent interactions [24]. Isotherm constants A and B can be determined from a plot of q_e vs C_e shown in Fig 9a & b. The correlation coefficients R^2 value of (0.821 & 0.781) for 100 ppm and 150 ppm respectively. The comparison of the linear form of Langmuir, Freundlich and Tempkin isotherms on the adsorption of CV onto BTSP can be made with the help of Table 3. It showed that the correlation Langmuir isotherm is much better (0.999 & 0.997) for 100 ppm and 150 ppm than that of Freundlich isotherm model (0.832 & 0.848) for 100 ppm and 150 ppm and Tempkin model (0.821 & 0.781) for 100 ppm and 150 ppm. Moreover Langmuir isotherm was the best fitted than other models. It proved the mono layer adsorption takes place in the adsorption of CV onto BTSP.

CONCLUSION

The results of the present investigation suggested that the BTSP might be promising low cost adsorbent for the removal of Crystal violet from waste water. There is no report on the adsorptive removal of dye solution by activated carbon prepared from *Bauhenia tomentosa*. The results proved that it can be utilized as a natural adsorbent in wastewater treatment as an alternate for commercial adsorbent.

Authors declares no conflict of interest

REFERENCES

1. R. Ahmad, "Studies on adsorption of crystal violet dye from aqueous solution onto coniferous pinus bark powder." J. Hazard, Mater., 171 (1), 767–773, 2009.





Poonkodi et al.,

2. G. Annadurai, R.S. Juang and J. Lee, "Use of cellulose based wastes for adsorption of dyes from aqueous solutions" *J. Hazard Mater.*, 892, 263-274, 2002.
3. S. Arivoli S and M. "Hema Comparative Study on the Adsorption Kinetics and Thermodynamics of Dyes onto Acid Activated Low Cost Carbon" *Inter. J. Phy. Sci.*, 10 17 (2007).
4. Y. Benjelloun, Y. Miyah Idressi, S. Boumchita S., A. El Ouali Lalami, and F. Zerrouq. "Removal of Crystal Violet by wet oxidation with H₂O₂ over an Iron oxide catalyst synthesized from Fly Ash." *J Mater. Environ. Sci.*, 8 (7), 2259-2269 2017.
5. S. Chakraborty, S. Chowdhury, and P. D. Saha. "Adsorption of crystal violet from aqueous solution onto NaOH-modified rice husk" *Carbohydr. Polym.* 86 (4), 1533–1541, 2011.
6. Y. S. Ho, and G. McKay. "Pseudo second order model for sorption process." *Process Biochem.*, 34, 451-465, 1999.
7. Y. S. Ho, and G. McKay. "Kinetic models for the sorption of dye from aqueous solution by wood." *Trans. I Chem. E. B*, 76 183-191, 1998.
8. S. Lagergren, About the Theory of So-Called Adsorption of Soluble Substances. *Kungliga Svenska Vetenskapsakademiens Handlingar*, 24, 1-39, 1898.
9. J. H. Elovich, and E. D. Schulman. "Proceedings of the Second International Congress on Surface Activity". Academic Press, Inc., New York, 11, pp.253, 1959.
10. E. H. Gürkan, S. Çoruh and S. E. Evli. "Adsorption of lead and copper using waste foundry sand: statistical evaluation." *Int. J. Global Warming*, 14(2), 260-263, 2018.
11. Y. Ming Chen, T. Tsao, M. Wang. "Removal of Crystal Violet and Methylene Blue from Aqueous Solution using Soil Nano-Clays." *IPC BEE, IACSIT Press* 8, 2011.
12. P. Priya, R. Nithya, R. Anuradha, T. Kamachi. "Removal of Colour from Crystal Violet Dye using Low Cost Adsorbents." *International Journal of ChemTechResearch* 6(9), 4346-4351, 2014.
13. V. K. Verma and A. K. Mishra, "Removal of dyes using low cost adsorbents." *Indian J. Chem. Technol.*, 15, 140-145, 2008.
14. C. Namasivayam and S. Sumithra. "Removal of direct red 12B and methylene blue from water by adsorption onto Fe (III)/Cr (III) hydroxide, an industrial solid waste." *J. environ management* 74(3), 207-215, 2005.
15. S. Senthilkumar, P. Kalaamani and C. V. Subburaam. "Liquid phase adsorption of crystal violet onto activated carbons derived from male flowers of coconut tree." *J. Hazard Mater*, 136, 800–808, 2006.
16. P. Mohandass and T. K. Ganesan. "Removal of Dyes Using Leaves of *Morinda Pubescens* a Low Cost Green Adsorbents." *Int. J. Innovative Res. Sci. Eng. and Technol*, 5(2), 1565-1571, 2016.
17. A. Saeed, M. Sharif and M. Iqbal. "Application potential of grapefruit peel as dye sorbent: Kinetics, equilibrium and mechanism of crystal violet adsorption." *J. hazard mater*, 179(1), 564-572, 2010.
18. M. R. Unnithan, V. P. Vinodan and T. S. Anirudhan. "Ability of iron(III) loaded carboxylated polyacrylamide-grafted sawdust to remove phosphate ions from aqueous solution and fertilizer industry wastewater: Adsorption kinetics and isotherm studies." *J. Appl. Polym. Sci.*, 84, 2541–2553, 2002.
19. S. Coruh, E. F. Gurkan. "Adsorption Of Crystal Violet From Aqueous Solutions Using Pirina." *International Journal of Advances in Science Engineering and Technology*, Vol-4,3, spl-2, 2016.
20. K. Sakthivel, I. Arockiaraj, C. Kannan and S. Karthikeyan. "Film- Pore diffusion Modeling for Sorption of Azo Dye on to One and Three Dimensional Nano Structured Carbon Nano Materials from *Jatropha Curcas*." *J. Environ. Nanotechnol*, 2(2), 66-75, 2013.
21. G. H. Sonawane and V. S. Shrivastava. "Kinetics of decolorization of malachite green from aqueous medium by maize cob (*Zea mays*): an agricultural solid waste." *Desalination*, 247, 430-441, 2009.
22. B. H. Hameed, A. T. M. Din, A. L. Ahmad. "Adsorption of methylene blue onto bamboo-based activated carbon: Kinetics and equilibrium studies." *Journal of Hazardous Materials*, 141(3), 819-825, 2007.
23. M. Makeswari and T. Santhi. "Removal of Malachite Green dye from Aqueous Solutions onto microwave assisted zinc chloride chemical activated epicarp of *Ricinus Communis*." *J. Water Res. Protect.*, 5, 222-238, 2013.





Poonkodi et al.,

Table 1: Data for the elements presented in BTSP

Element	App conc.	Intensity cornn.	Weight%	Weight% sigma	Atomic%
C	30.65	1.1308	60.75	1.16	67.75
O	7.84	0.4645	37.80	1.17	31.64
S	0.62	0.9634	1.45	0.18	0.61
Totals					100.00

Table 2: Comparison of the correlation coefficients of kinetic parameters for the adsorption of CV onto BTSP

Kinetic model	Concentration (ppm)	Parameters	BTSP
Pseudo first-order	100ppm	$K_1(\text{min}^{-1})$	0.0112
		$q_e(\text{mg/g})$	38.4615
		R^2	0.944
	150ppm	$K_1(\text{min}^{-1})$	0.0104
		$q_e(\text{mg/g})$	41.6666
		R^2	0.939
Pseudo second -order	100ppm	$K_2(\text{min}^{-1})$	0.0017
		$q_e(\text{mg/g})$	250
		R^2	0.999
	150ppm	$K_2(\text{min}^{-1})$	0.0008
		$q_e(\text{mg/g})$	500
		R^2	0.973
Elovich model	100ppm	$A_E(\text{Mg/min})$	0.0311
		$b(\text{g/mg})$	68.36
		R^2	0.973
	150ppm	$A_E(\text{Mg/min})$	0.0116
		$B(\text{g/mg})$	63.80
		R^2	0.944
Intra particle diffusion	100ppm	K_{dif}	0.3825
		C	106.5
		R^2	0.915
	150ppm	K_{dif}	0.2490
		C	38.52
		R^2	0.960

Table 3: Comparison of the correlation coefficient parameters for the isotherm adsorption

Isotherms	Concentration(ppm)	Parameters	BTSP
Langmuir isotherm	100ppm	$K_1(\text{Lmg}^{-1})$	0.2032
		$Q_m(\text{m}g\text{g}^{-1})$	40.00
		R^2	0.999
	150ppm	$Q_m(\text{m}g\text{g}^{-1})$	43.47
		R^2	0.997
Freundlich isotherm	100ppm	$1/n$	0.1270
		$K_f(\text{m}g\text{g}^{-1})$	1.8757
		R^2	0.832
	150ppm	$1/n$	0.1830
		$K_f(\text{m}g\text{g}^{-1})$	2.0218
		R^2	0.848





Poonkodi et al.,

Tempkin isotherm	100ppm	α (Lg-1)	0.363
		β (mgL-1)	4.107
		R ²	0.821
		β (g/mg)	4.838
		R ²	0.781

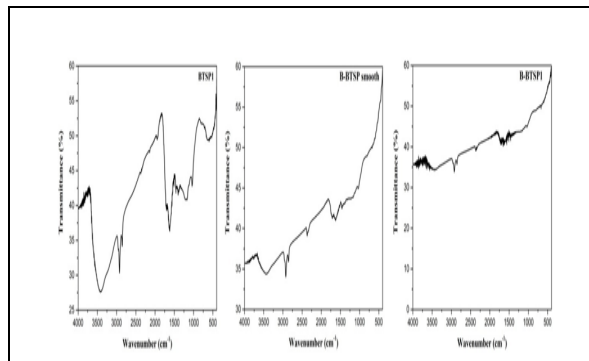


Fig.1.FT-IR analysis of BTSP adsorbent raw powder(1a), before(1b) and after (1c) adsorption of CV dye

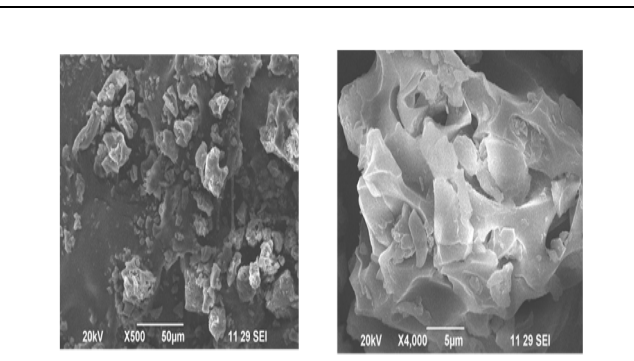


Fig. 2. SEM image of the BTSP before and after adsorption

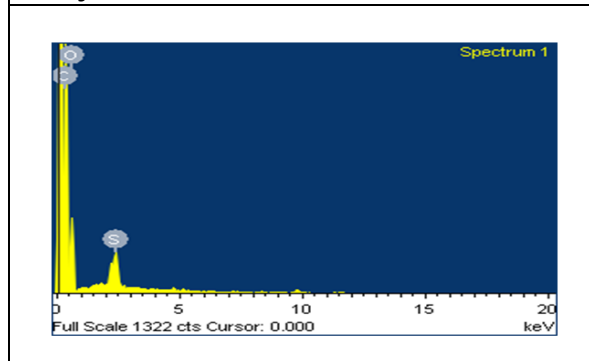


Fig. 3. EDX spectrum of BTSP

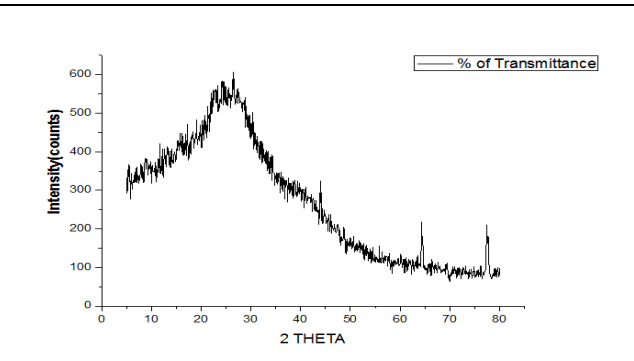


Fig. 4. XRD Pattern of BTSP

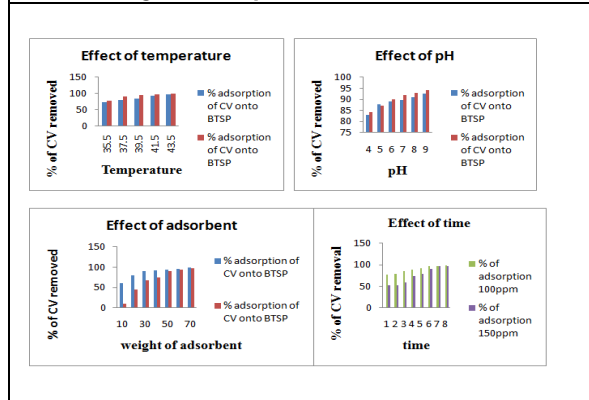


Fig. 5a, 5b,5c & 5d. Effect of pH, Temperature, dose and time on the adsorption of CV onto BTSP

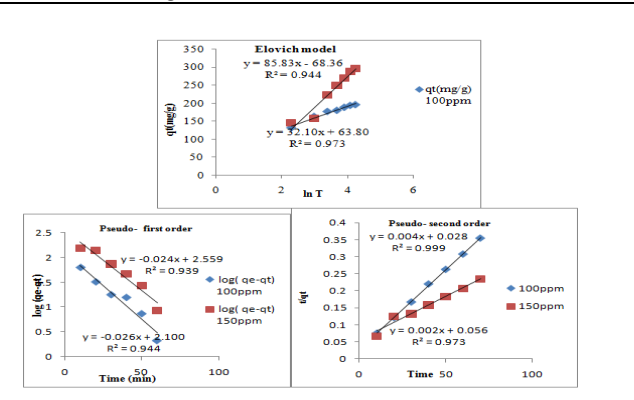


Fig. 6a, 6b & 6c. Pseudo First order, second order and Elovich model kinetics for CV onto BTSP





Poonkodi et al.,

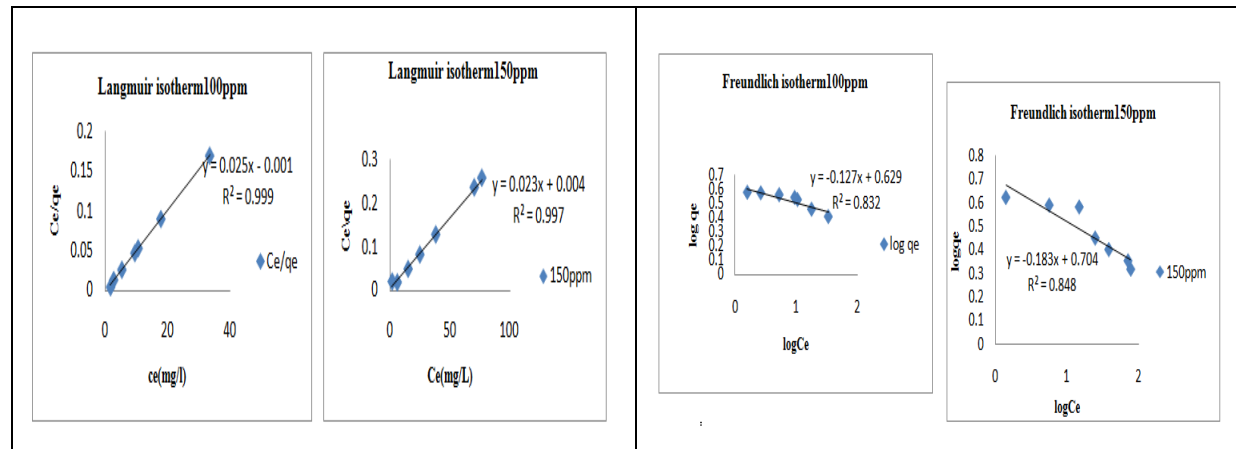


Fig. 7a.&b Langmuir isotherm plot for 100 & 150 ppm for adsorption CV onto BTSP

Fig. 8. a & b. Freundlich isotherm plot for 100 & 150 ppm for adsorption CV onto BTSP fruit shell

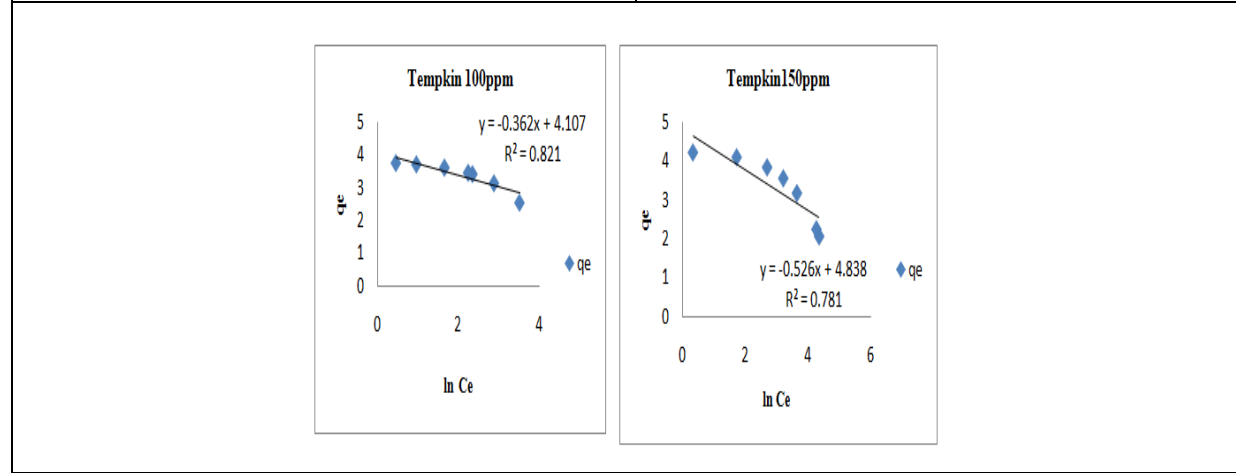


Fig. 9. a&b. Temkin isotherm plot for 100 & 150 ppm for adsorption CV onto BTSP

